The study of electrical characteristics of heterojunction based on ZnO nanowires using ultrahigh-vacuum conducting atomic force microscopy

J. H. He[a] and C. H. Ho
Institute of Photonics and Optoelectronics and Department of Electrical Engineering, National Taiwan University, Taipei, 106 Taiwan, Republic of China

(Received 30 August 2007; accepted 15 November 2007; published online 5 December 2007)

The electrical performances of the heterojunction of *n*-ZnO nanowires with *p*-Si substrate at the nanometer scale have been characterized using an ultrahigh-vacuum conducting atomic force microscopy. Compared with the expected values of 1.0–2.0 reported in *p-n* junction in the previous studies, the abnormally high diode ideality factor ($\geqslant 2$) was obtained. It elucidates that a ZnO–Si *p-n* junction can be modeled by a series of diodes, the actual ZnO–Si junction diode and two Schottky diodes at the metal/ZnO and metal/Si junctions. The tunneling across *p-n* junction would also play a role in the externally measured high ideality factor. © *2007 American Institute of Physics*.
[DOI: 10.1063/1.2821831]

ZnO-based materials and devices have attracted substantial interest since ZnO has several potential advantages, such as the commercial availability of bulk single crystals, wide band gap, and the large exciton binding energy (~60 meV compared to ~25 meV for GaN).[1] The fabrication of effective ZnO *p-n* homojunction remains to be accomplished since ZnO is intrinsically *n*-type materials, and the growth of reproducible high-quality *p*-type ZnO is not achieved yet. As an alternative way, ZnO-based heterojunctions are being investigated for realizing device application.[2–4] In addition, the nanodevices based on ZnO nanowires (NWs), such as optically pumped nanolaser,[5] nanogenerator,[6] acoustic resonator,[7] piezoelectric gated diode,[8] field emitter,[9] chemical sensor,[10] and UV detector,[11] have been demonstrated due to the combination of structural, semiconducting, and piezoelectric properties of ZnO nanomaterials. Recently, the studies of the NW-based heterojunctions, such as *n*-ZnO NWs/*p*-GaN (Ref. 12) and *n*-ZnO/*p*-Si,[13,14] have been fabricated to investigate their electrical and optoelectronic properties, including the current-voltage (*I-V*), electroluminescent, and photoresponse measurements. Therefore, it is essential to gain a better insight into the electrical properties of the *p-n* heterojunction diode above.

According to the Sah-Noyce-Shockley theory,[15] the forward current in a *p-n* junction is dominated by recombination of minority carriers injected into the neutral regions of the junction. This kind of transport gives an ideality factor of 1.0. Recombination of carriers in the space-charge region, mediated by recombination centers located near the intrinsic Fermi level, results in an ideality factor of 2.0. However, the Sah-Noyce-Shockley model cannot account for ideality factors greater than 2.0 found in *p-n* junction.

In the present study, we have demonstrated the electrical performances of a heterojuction of *n*-ZnO NW with *p*-Si at the nanoscale using ultrahigh-vacuum conducting atomic force microscopy (C-AFM). To analyze measured electrical transport, we propose an explanation for the high ideality factor in ZnO–Si heterojunciton. It elucidates that a ZnO–Si *p-n* junction can be modeled by a series of diodes, the actual ZnO–Si junction diode and two Schottky diodes at the metal/ZnO and metal/Si junctions. A theoretical model on the effective ideality factor of a system of junctions is in agreement with the experimental data.

Fabrication of heterojunction *n*-ZnO/*p*-Si has been reported elsewhere.[13] Electrical measurements of heterojuctions of ZnO NWs/*p*-Si substrate were made using a standard commercial instrument (Omicron ultrahigh-vacuum variable temperature AFM). The pressure in the analysis chamber was below 5×10^{-11} mbar during the experiments. C-AFM measurements were carried out in contact mode using silicon cantilevers with constant loading forces in the range between 30 and 50 nN. The AFM tip was precoated with a PtIr layer, provided by the manufacturer (Nanosensors), and subsequently coated with a Ti/Au (30 nm/30 nm) film by electron beam evaporation for obtaining Ohmic contact between Ti and ZnO. The 30-nm-thick Pt was also sputtered onto the back side of the *p*-type Si substrate to obtain Ohmic contact. C-AFM tip is used to apply voltage and measure the current through the NW and Si substrate.

Under controlled experimental condition, ZnO NW arrays were grown on $Al_2O_3(11-20)$ substrate surface using Au as catalyst. The phase of NWs is hexagonal wurtzite-structured ZnO, and the growth direction of ZnO NW arrays is [0001] direction.[16]

An undoped ZnO NW usually exhibits *n*-type characteristics due to presence of zinc interstitials and/or oxygen vacancies. The *I-V* curves analyzed by two-electrode transport measurement for a ZnO NW deposited on an insulating layer and connected by a pair of Ti/Au electrodes as an Ohmic metal electrode, and a boron-doped Si substrate connected by a pair of Pt electrodes as an Ohmic electrode for *p*-type Si indicate that the linear trend shows the establishment of Ohmic contacts, as shown in Fig. 1. The detailed method to deposit metal electrodes onto a NW has been reported elsewhere.[17] After ensuring Ohmic characteristics for the metal-semiconductor interface, *I-V* characteristics of the Si/ZnO heterojunction could be measured further. After fabricating heterojunction based on ZnO NWs, electrical measurements were performed in C-AFM. The C-AFM probe was positioned directly onto the NW and used to apply voltage and measure the current through the NW and Si substrate, as shown in Fig. 2(a). Previous study indicates good

[a]Electronic mail: jhhe@cc.ee.ntu.edu.tw.

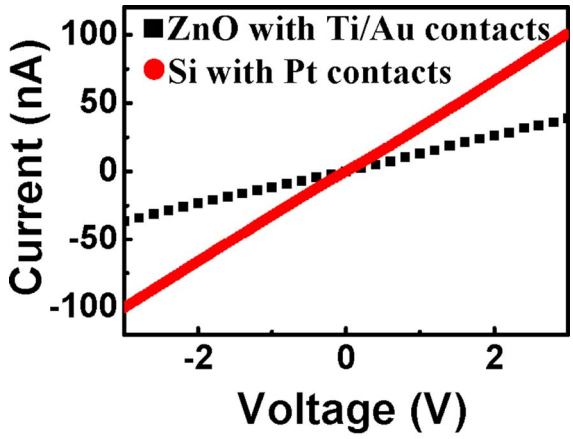

FIG. 1. (Color online) *I-V* characteristics of the ZnO NW with Ti/Au contacts and Si with the Pt contacts showing Ohmic characteristics.

contact between the ZnO NWs and Si substrate and uniformity in electrical performance along ZnO NW.[13] The inset of Fig. 2(a) shows that a pronounced rectifying diodelike behavior was observed, while the AFM tip was used to contact the ZnO NW and to apply voltage. An energy band diagram is drawn in Fig. 2(b) based on individual band structures to explain the behavior of *n*-ZnO/*p*-Si heterojunction. It is known that the energy gaps (E_g) for ZnO and Si are 3.27 and

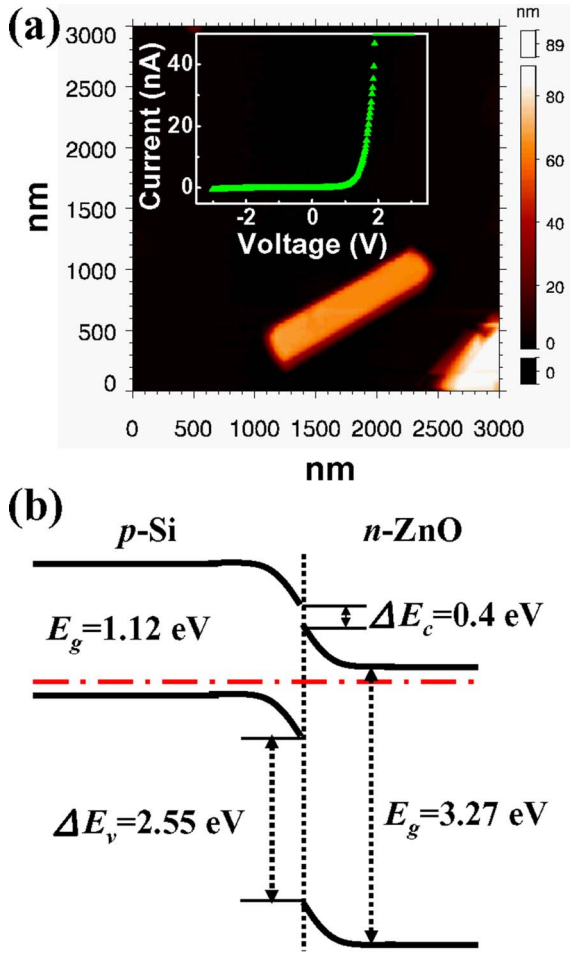

FIG. 2. (Color online) (a) AFM topography image of heterojunction diode based on ZnO nanowires (inset: electron transport characteristics of ZnO/Si heterojunction). (b) The energy band diagram of the heterojunction *n*-ZnO/*p*-Si at zero voltage bias.

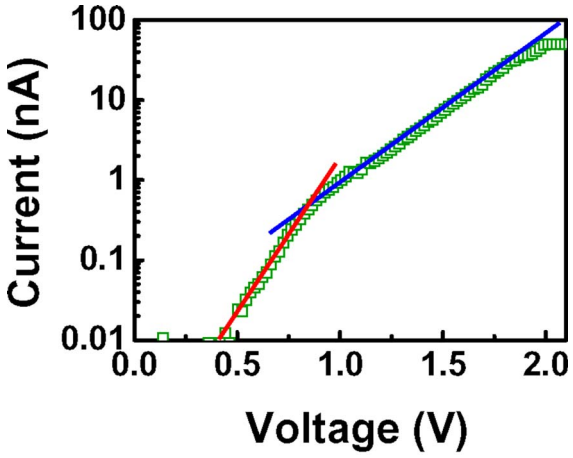

FIG. 3. (Color online) A logarithm plot of current vs bias in the inset of (b). The curve can be simulated with diode ideality factors $n=4.28$ in the range from 0.46 to 0.85 V and $n=9.44$ in the range from 0.85 to 1.89 V.

1.12 eV, respectively. The valence band offset is much larger than the conduction band offset. The higher barrier in the valence band prevents the holes' movement. Therefore, the conductive property of this heterojunction is determined by the electrons in the conduction band. However, these arguments are for the ideal case, and direct measurements are required to determine the exact band structure of the heterojunction.

The ideality of the diode can be determined from the forward-biased characteristic. Figure 3 is a semilogarithmic plot of current versus forward bias of the inset of Fig. 2(a). The forward-biased current is

$$I = I_S\left[\exp\left(\frac{eV}{nkT}\right) - 1\right], \tag{1}$$

$$n = \frac{e}{kT}\frac{dV}{d\ln I}, \tag{2}$$

where n is the ideality factor which is a quantity for describing the deviation of the diode from an ideal *p-n* junction, for which $n=1$, I_S is the reverse saturation current, V is the forward-biased voltage, k is the Boltzmann constant, and T is the absolute temperature. Fitting of the experimental data using Eq. (1) yields n values. The values of n obtained for the *p*-Si/*n*-ZnO heterojunction were found to be approximately 4.28 at voltages ranging from 0.46 to 0.85 V and approximately 9.44 at voltages ranging from 0.85 to 1.89 V. According to the Sah-Noyce-Shockley theory,[15] the values of the ideality factor are around 1.0 at a low voltage and up to 2.0 at a higher voltage. However, the theoretical model cannot account for ideality factors greater than 2.0 found in the present study. This can be attributed to the presence of nonlinear metal-semiconductor contact.[18–20] The heterojunction diode can then be modeled by a series connection of diodes or resistances in a dissimilar bias range: the actual *p*-type Si/*n*-type ZnO heterojunction diode, the contact resistance between metal/*p*-type Si (or Schottky diode), and the contact resistance between metal/*n*-type ZnO (or Schottky diode). Although the two metal-semiconductor junctions of a diode ideally have Ohmic characteristics, the contacts could exhibit nonlinear characteristics in the interim bias voltage range. As forward bias just applied, it is *p*-type Si/*n*-type ZnO heterojunction diode with two ideal metal-semiconductor contact

resistances. In the limit of high contact resistance, the metal-semiconductor contact could be considered as reverse-biased Schottky contact in the interim bias voltage range.[21] Therefore, it could be a p-Si/n-ZnO heterojunction, metal/p-type Si Schottky diode, and/or metal/n-type ZnO Schottky diode in the interim bias voltage range (<1.89 V). These three diodes have different values of reverse saturation current and ideality factors. A summation of three diodes could be used to model the various conduction mechanisms. As the external current and voltage are given by I and $V=\Sigma V_i$, the I-V characteristic of the structure is given by

$$V=\sum_i V_i=\sum_i\left[n_i\left(\frac{kT}{e}\right)\ln I-n_i\left(\frac{kT}{e}\right)\ln I_{\mathrm{Si}}\right], \tag{3}$$

where the factor I_{Si} is the reverse saturation current of each junction, V_i is the voltage at each junction, and n_i is the ideality factor of each junction. We assume that the diode voltages are $V_i \gg kT/e$, so that $\exp(eV/nkT)\gg 1$. Rearrangement of the terms in the above equation yields

$$\ln I=\frac{(e/kT)}{\Sigma_i n_i}V+\frac{\Sigma_i n_i \ln I_{\mathrm{Si}}}{\Sigma_i n_i}. \tag{4}$$

In Eq. (4), the second summation is a constant, since we consider only the linear region of the $\ln(I)$-V characteristic, where n_i are constants. According to Eq. (4), the externally measured ideality factor is a sum of the ideality factors of the individual rectifying junctions. This result can be expressed as $n=\Sigma_i n_i$, where n_i represent the ideality factors of p-Si/n-ZnO heterojunction, metal/p-type Si junction, and metal/n-type ZnO junction. Accordingly, it is evident that the ideality factor of the diode $\gg 2$ can be measured. In addition, since two metal-semiconductor contacts (metal/ZnO and metal/Si) could be turned into reverse-biased Schottky contact at different bias voltages, two slopes, which stands for two n values, were obtained at bias voltages ranging from 0.46 to 1.89 V. As shown in Fig. 3, in the bias voltage range greater than 1.89 V, the equivalent circuit of the device turns out to be three resistances instead of the combination of p-Si/n-ZnO heterojunction, metal/p-type Si Schottky diode, and metal/n-type ZnO Schottky diode, since the I-V characteristic in the inset of Fig. 2(a) is linear when bias voltage is higher than 1.89 V.

Moreover, the high ideality factors ($n\gg 2.0$) in GaN-based light-emitting diodes[22,23] were attributed to deep-level-assisted tunneling[24] across p-n junction, since the measurement of the I-V behavior demonstrated a temperature independent semilogarithmic slope, which is characteristic of deep-level-assisted tunneling current rather than diffusion or space-charge recombination current where the ideality factor n varies between 1.0 and 2.0. Therefore, in addition to the sum of the ideality factors of the individual rectifying junctions (i.e., the actual ZnO–Si junction diode and two Schottky diodes at the metal/ZnO and metal/Si junctions), the tunneling across p-n junction would also play a role in the externally measured high ideality factor in this study.

In summary, we have demonstrated the electrical performances of a heterojuction of n-ZnO NW with p-Si substrate at the nanoscale using C-AFM. To gain a better understanding of the measured electrical properties of the p-n heterojunction diode above, the theoretical model was proposed to analyze the anomalously high ideality factor of the prepared p-n junction diode. The externally measured ideality factor of Si/ZnO diode is the sum of the ideality factors of the individual rectifying junction. The tunneling across Si/ZnO p-n junction would also play a role in the externally measured high ideality factor.

The research was supported by the National Science Council under Grant No. NSC 96-2112-M-002-038-MY3 and NSC 96-2622-M-002-002-CC3.

[1] U. Ozgur, Y. I. Alivov, C. Liu, A. Teke, M. A. Reshchikov, S. Dogan, V. Avrutin, S. J. Cho, and H. Morkoc, J. Appl. Phys. **98**, 041301 (2005).
[2] I. S. Jeong, J. H. Kim, and S. Im, Appl. Phys. Lett. **83**, 2946 (2003).
[3] J. D. Ye, S. L. Gu, S. M. Zhu, W. Liu, S. M. Liu, R. Zhang, Y. Shi, and Y. D. Zheng, Appl. Phys. Lett. **88**, 182112 (2006).
[4] Y. I. Alivov, Ü. Özgür, S. Dogan, D. Johnstone, V. Avrutin, N. Onojima, C. Liu, J. Xie, Q. Fan, and H. Morkoç, Appl. Phys. Lett. **86**, 241108 (2005).
[5] M. H. Huang, S. Mao, H. Feick, H. Q. Yan, Y. Y. Wu, H. Kind, E. Weber, R. Russo, and P. D. Yang, Science **292**, 1897 (2001).
[6] Z. L. Wang and J. H. Song, Science **312**, 242 (2006).
[7] B. A. Buchine, W. L. Hughes, F. L. Degertekin, and Z. L. Wang, Nano Lett. **6**, 1155 (2006).
[8] J. H. He, C. L. Hsin, J. Liu, L. J. Chen, and Z. L. Wang, Adv. Mater. (Weinheim, Ger.) **19**, 781 (2007).
[9] Y. B. Li, Y. Bando, and D. Golberg, Appl. Phys. Lett. **84**, 3603 (2004).
[10] Z. Y. Fan, D. W. Wang, P. C. Chang, W. Y. Tseng, and J. G. Lu, Appl. Phys. Lett. **85**, 5923 (2004).
[11] J. H. He, Y. H. Lin, M. E. McConney, V. V. Tsukruk, Z. L. Wang, and G. Bao, J. Appl. Phys. **102**, 084303 (2007).
[12] W. I. Park and G. C. Yi, Adv. Mater. (Weinheim, Ger.) **16**, 87 (2004).
[13] J. H. He, S. T. Ho, T. B. Wu, L. J. Chen, and Z. L. Wang, Chem. Phys. Lett. **435**, 119 (2007).
[14] R. Ghosh and D. Basaka, Appl. Phys. Lett. **90**, 243106 (2007).
[15] C. Sah, R. N. Noyce, and W. Shockley, Proc. IRE **45**, 1228 (1957).
[16] H. He, C. S. Lao, L. J. Chen, D. Davidovic, and Z. L. Wang, J. Am. Chem. Soc. **127**, 16376 (2005).
[17] C. L. Hsin, J. H. He, C. Y. Lee, W. W. Wu, P. H. Yeh, L. J. Chen, and Z. L. Wang, Nano Lett. **7**, 1799 (2007).
[18] C. X. Wang, G. W. Yang, H. W. Liu, Y. H. Han, J. F. Luo, C. X. Gao, and G. T. Zou, Appl. Phys. Lett. **84**, 2427 (2004).
[19] J. M. Shah, Y. L. Li, T. Gessmann, and E. F. Schubert, J. Appl. Phys. **94**, 2627 (2003).
[20] C. X. Wang, G. W. Yang, T. C. Zhang, H. W. Liu, Y. H. Han, J. F. Luo, C. X. Gao, and G. T. Zou, Diamond Relat. Mater. **12**, 1548 (2003).
[21] J. C. Ranuarez, F. J. G. Sanchez, and A. Ortiz-Conde, Solid-State Electron. **43**, 2129 (1999).
[22] H. C. Casey, Jr., J. Muth, S. Krishnankutty, and J. M. Zavada, Appl. Phys. Lett. **68**, 2867 (1996).
[23] P. Perlin, M. Osinski, P. G. Eliseev, V. A. Smagley, J. Mu, M. Banas, and P. Sartori, Appl. Phys. Lett. **69**, 1680 (1996).
[24] D. J. Dumin and G. L. Pearson, J. Appl. Phys. **36**, 3418 (1965).